New Down-Converter for UV-Stable Perovskite Solar Cells: Phosphor-in-Glass

Hee-Suk Roh [a,b], Gill Sang Han [a], Seongha Lee [a], Sanghyun Kim [b], Sungwoo Choi [b], Chulsoo Yoon [b], and Jung-Kun Lee [a,*]

[a] Department of Mechanical Engineering & Material Science, University of Pittsburgh, PA 15261, United States

[b] LED business, Samsung Electronics Co. LTD., Yongin, Republic of Korea

[*] Corresponding author: Jung-Kun Lee (E-mail address: jul37@pitt.edu)

Abstract

Degradation of hybrid lead halide perovskite by UV light is a crucial issue that limits the commercialization of lead halide perovskite solar cells (PSCs). To address this problem, phosphor-in-glass (PiG) is used to convert UV to visible light. Down-conversion of UV light by PiG dramatically increases UV-stability of PSCs and enables PSCs to harvest UV light that is currently wasted. Performance of PSCs with PiG layer does not change significantly during 100 hour-long UV-irradiation, while conventional PSCs degrade quickly by 1 hour-long UV-irradiation. After 100 hour long UV-irradiation, power conversion efficiency of PSCs with PiG is 440 % larger than that of conventional PSCs. This result points a direction toward PSCs which are very stable and highly efficient under UV light.

Graphical abstract

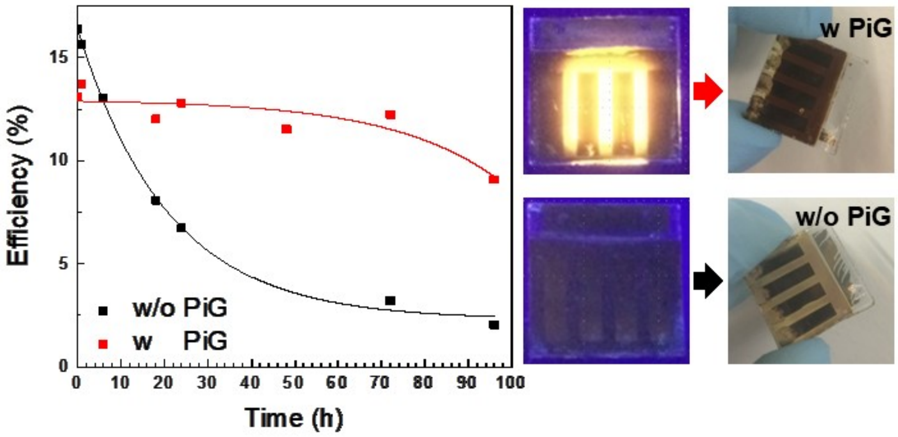

Keywords: hybrid lead halide perovskite, light stability, phosphor-in-glass, luminescent down-converter

1. Introduction

Hybrid lead halide perovskite solar cells (PSCs) have been intensively investigated over the past several years as a next generation solar cells. Certified power conversion efficiency (PCE) of PSCs has increased to 22.7 % that is the highest among emerging solar cells. [1–5] Additional strengths of PSCs are low material cost and facile fabrication process. [6,7] However, PSCs degrade quickly by exposure to UV light, humidity or heat. This degradation problem limits the commercialization of PSCs. [8–10] Though the instability of PSCs by humidity and heat attracts a considerable amount of interest, [11–13] the effect of UV light on TiO_2-based PSCs has been relatively neglected. [14] Current solutions to UV light problem are to remove UV light by inserting an additional UV filter or replace photocatalytic TiO_2 with less photoactive semiconductor such as $BaSnO_3$. However, removal of UV component reduces power of incident solar light and TiO_2 layer is still known the best electron transport layer for high efficiency PSCs.

If UV component of solar light is converted to visible light, UV degradation of PSCs can be addressed without sacrificing PCE of PSCs. Several groups have demonstrated down-conversion of UV light to visible light by nanosize phosphors. [15-17] However, nanosized phosphors used in the down-conversion have relatively lower photostability due to a change in an oxidation state by excitation light. [18,19] This lowers a down-conversion efficiency of the phosphor layer. Phosphor-in-glass (PiG) is a composite consisting of phosphor particles and glass matrix. Phosphors in PiG convert UV or blue light to green or yellow light, which is called down-conversion. In high-power light emitting diode (LED) devices PiG covers an active part of LED and has a dual function of down-conversion and encapsulation. [20-22] Since phosphor particles are well isolated from ambience by thermally conductive glass matrix, the optical property of phosphor particles is well maintained in harsh environment (i.e. strong UV light radiation and high temperature). Moreover, the photoluminescence properties of PiG can be simply controlled by changing phosphors mixed in PiG. It is expected that the efficiency and stability of PSCs are improved at the same time by applying the mixture of up-converting and down-converting phosphors to PiG due to the ability of up-converting phosphor which converts over 800 nm of light to valuable visible light. [23]

In this study, we report that the down-conversion ability of PiG improves the stability and PCE of PSCs. Given that PiG is already mass-produced for LED industry, a thin PiG plate can easily replace a glass substrate of PSCs or be attached to a glass substrate of PSCs. If such a solar cell with the thin PiG is illuminated from a PiG side, UV light is converted to visible light before the photocatalytic reaction of TiO_2 is activated. We chose PiG containing green $Lu_3Al_5O_{12}:Ce^{3+}$ and orange-SiAlON:Eu^{2+} phosphors, since this endures high light intensity and does not emit UV light at all. Therefore, PiG prevents underlying PSCs from being exposed to UV light. It is found that the down-conversion of PiG increases incident photon to current efficiency (IPCE) of fresh PSCs from 30 % to 53 % at the wavelength of 320 nm. After 100 hour-long UV light illumination, PCE of PSCs with PiG at AM 1.5G illumination is 440 % larger than that of conventional PSCs. These results indicate that implementation of PiG into PSCs is an effective way to protect PSCs from UV light without deteriorating PCE.

2. Experimental

Materials

Commercially available PiG was provided by LED business, Samsung Electronics. Green $Lu_3Al_5O_{12}:Ce^{3+}$ and orange α-SiAlON:Eu^{2+} phosphors were embedded in the glass matrix. Phosphors of average diameter 18 µm were mixed with low temperature glass frits (YEK Glass Co., LTD.) with a volume fraction of 1:9. A mixture was shaped into a plate through a tape casting method and sintered at 600 °C in air.

Fabrication of perovskite solar cells

FTO substrate was cleaned in acetone, deionized (Di) water, and ethanol. TiO_2 blocking layer (bl-TiO_2) was spin-coated on FTO substrate by using prepared 0.5 M titanium diisopropoxide bis-(acetylacetonate) in 1-butanol at 4000 rpm for 30 s. The mesoporous-TiO_2 nanoparticle (mp-TiO_2 NP) as electron transport layer (ETL) was spin-coated onto the bl-TiO_2/FTO substrate at 5000 rpm for 30 s by using diluted TiO_2 paste in ethanol (1:5.5 wt%, sharechem). And then, the substrate was annealed at 500 °C for 30 min. After cooling, the substrate was dipped into $TiCl_4$ solution for 30 min at 70 °C, subsequently, the substrate was rinsed with Di-water for 5 min and annealed in the box furnace at 500 °C for 30 min.

Perovskite ($CH_3NH_3PbI_3$) layer was deposited by using adduct method, as previously reported. [24] To prepared $CH_3NH_3I•PbI_2•DMSO$ solution, 1.0 M PbI_2, CH_3NH_3I, and DMSO (1:1:1 molar ratio) was dissolved in N,N-dimethylformamide (DMF) solvent for 30 min. And then, $CH_3NH_3I•PbI_2•DMSO$ solution was deposited onto the mp-TiO_2/bl-TiO_2/FTO substrate at 4000 rpm for 25 s and diethyl ether was dropped onto the substrate in 10 s. After that, the substrate was annealed at 65 °C for 3 min and 100 °C 10 min. The hole transport layer was spin-coated onto the perovskite/ mp-TiO_2/bl-TiO_2/FTO by mixing of spiro-OMeTAD in chlorobenzene (36 mg ml^{-1}), 14.4 ml of 4-tert-butylpyridine, and 8.8 ml of lithium-bis(trifluoro-methanesulphonyl)-imide salt (Li-TFSI) in acetonitrile (360 mg ml^{-1}). Finally, Au as a top electrode was deposited by using e-beam evaporator with 0.3 Å s^{-1} deposition rate.

Characterization of PiG and solar cells

Photoluminescence (PL) and decay time measurements were performed using spectrofluorometer (QuantaMaster, PTI). Excitation and Emission spectra were measured at 350 - 500 nm and 450 - 680 nm, respectively. A scan rate was 1 nm s^{-1}. Photostability of PiG was monitored at 560 nm under 365 nm of excitation. Reflectance and transmittance of PiG plate was examined using UV/Vis spectrophotometer (Lambda-55, Perkin Elmer). An integrating sphere was used to measure diffuse reflectance and transmittance. The J-V curve characteristics of the PSCs with active area of 0.14 cm^2 were measured by using potentiostat (CHI660C, CH Instrument) under AM 1.5G illumination.

Stability Test

Figure 1 shows a schematic on the stability test of PSCs with and without PiG plate. Filtered UV lamp (VL-215.LC, Vilber Lourmat) of 78 mW cm^{-2} was used to accelerate the degradation of PSCs. As shown in Figure 1, UV light of 365 nm wavelength was irradiated from the glass side of PSCs in airwith 25-40 % of humidity. To convert UV light to visible light, 200 μm thick PiG plate was placed on the surface of glass in a part of tested samples. Performance of UV-irradiated PSCs was measured at AM 1.5G illumination as a function of UV irradiation time.

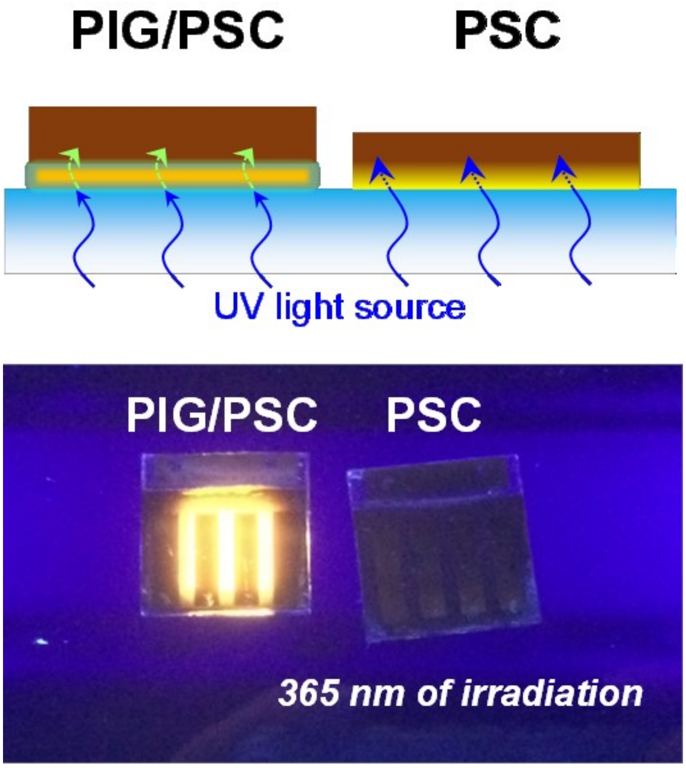

Figure 1. Top) a schematic on the stability test of PSCs with and without PiG plate; a PiG plate is placed between UV light source and PSC, bottom) photos of PiG/PSC and only PSC under UV radiation: emission of PiG is observed.

3. Results and Discussions

XRD patterns of PiG in Figure S1(a) testifies that $Lu_3Al_5O_{12}$ and α-SiAlON phosphors are mixed in PiG. The intensity of α-SiAlON phase is relatively small due to the small amount in PiG (wt.% ratio of $Lu_3Al_5O_{12}$:α-SiAlON = 9:1). SEM images in Figure S1(b) show that PiG has smooth surface with 200 μm thickness. Figure S1(c) shows photoluminescence (PL) emission and excitation spectra of PiG plate. Down-conversion of UV light to visible light by PiG is clearly observed in Figure S1(c). PL excitation spectrum of PiG for the emission wavelength of 556 nm ranges from 300 to 500 nm. Excitation intensity dramatically decreases as the excitation wavelength gets longer than 500 nm. PiG emits broad yellow light and the emission spectrum ranges from 460 to 680 nm. Emission peak wavelength is 560 nm and its full width at half maximum is 105 nm. Transmittance and reflectance spectra of PiG plate are also shown in Figure S1(d). For red light (λ = 600 nm) which PiG does not absorb, transmittance and reflectance of 200 μm thick PiG plate is 85 and 15 %. Theoretical reflectance (R) at normal incidence angle is calculated by Fresnel equation,

$$R = \left|\frac{n_1 - n_2}{n_1 + n_2}\right|^2 \qquad (1)$$

where n_1 and n_2 are refractive index of air and PiG. Since the refractive index of PiG is 1.8, the theoretical reflectance of smooth PiG surface is calculated as 8 %. A difference between measured reflectance (15 %) and theoretical reflectance (8 %) is due to backward scattering at the interface between phosphor particles and glass matrix. Light backscattering by embedded phosphor particles was also reported in phosphor-converted white light emitting diode (pc-LED). When blue light was incident upon $Y_3Al_5O_{12}:Ce^{3+}$ phosphor layer, 12 % of power was reflected through backscattering. [25]

Figure 2(a) shows J-V curve of fresh PSCs with and without PiG at AM 1.5G illumination. Short circuit current density (J_{SC}) of PSCs slightly decreases from 21.33 mA cm^{-2} to 17.29 mA cm^{-2} when PiG is added. Open circuit voltage (V_{OC}) and fill factor (FF) are almost same. Given that total reflectance at PiG plate surface and glass/phosphor interface is ~15%, J_{SC} is expected to decrease by 15 %. However, experimentally measured J_{SC} of PSCs with PiG is 81 % of that of PSCs without PiG. This is because the internal quantum efficiency of the down-conversion process is less than 100 %. Stokes shift process consumes a small portion of the incident energy and additional 4 % loss of J_{SC}

occurs. IPCE spectra of fresh PSCs with and without PiG are shown in Figure 2(b). While a small portion of incident energy is lost in the visible region through the down-conversion process, PiG clearly increases photocurrent of PSCs in the UV region. Generally, incident photon-to-current efficiency (IPCE) of PSCs is almost zero for deep UV light ($\lambda < 300$ nm). However, IPCE of PiG added PSCs increases to 20 - 55 % in UV regime (200 nm $< \lambda <$ 320 nm), since PiG converts UV light to visible light.

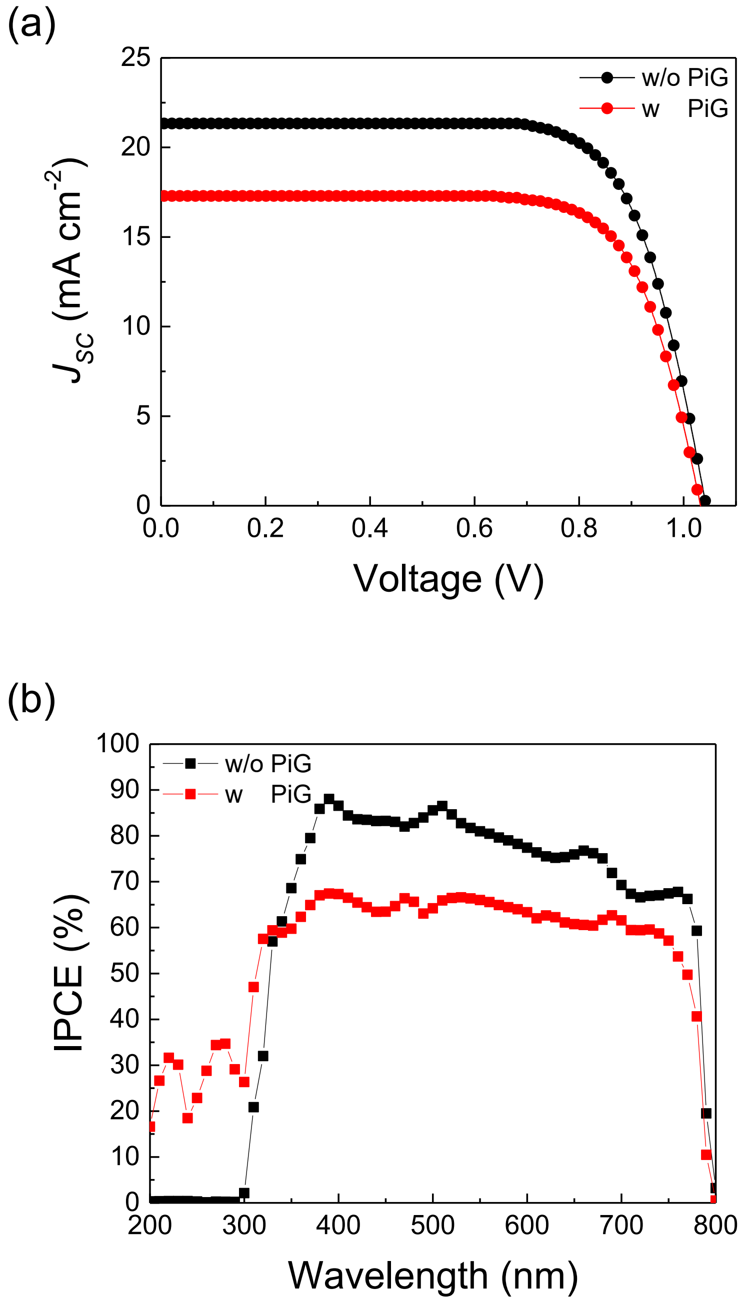

Figure 2. (a) *J-V* curve of PSCs and (b) IPCE without PiG and with PiG.

To examine the effect of PiG on UV stability, PSCs with and without PiG plate are irradiated with 365 nm UV light in air and a change in photovoltaic performance is evaluated. Figure 3 shows normalized efficiency, J_{SC}, V_{OC} and *FF* of PSCs as a function of 365 nm UV light irradiation time. J_{SC}, V_{OC} and *FF* of PSCs without PiG plate decrease by 40 – 60 % and PCE of PSCs after 100 hr - long UV irradiation is only 13 % of the initial PCE. In contrast, PSCs with PiG are stable under UV irradiation and PCE of 100 hr irradiate PSCs is 70 % of the initial PCE. Color of PSCs without PiG turns to pale brown after 100 hr-long UV irradiation, as shown in Figure 3(a). However, a color change PSCs is not observed when a solar cell is irradiated through PiG plate. A main reason for a decrease in PCE is decomposition of halide perovskite by UV light. TiO_2 is an excellent electron transport material and most commonly used in PSCs. In addition, TiO_2 nanoparticles can extract electrons from I^- through a photocatalytic reaction when TiO_2 is exposed to supraband gap photons (photon energy > 3.2 eV). Oxidation of iodide ion (I^-) subsequently causes decomposition of $CH_3NH_3^+$. Ito *et al.* proposed following decomposition reactions in UV light irradiated PSCs: [8]

$$2I^- \leftrightarrow I_2 + 2e^- \text{ [at the interface between } TiO_2 \text{ and } CH_3NH_3PbI_3] \quad (2)$$

$$CH_3NH_3^+ \leftrightarrow 3CH_3NH_2\uparrow + 3H^+ \quad (3)$$

$$I^- + I_2 + 3H^+ + 2e^- \leftrightarrow 3HI\uparrow \quad (4)$$

Decomposition of $CH_3NH_3^+$ is accelerated by the continuous elimination of H^+ through evaporation of HI in reaction (4). Consequently, $CH_3NH_3PbI_3$ transforms into PbI_2 and gas byproducts (CH_3NH_2, HI). [26] Since a small amount of PbI_2 can passivate defects inside $CH_3NH_3PbI_3$ layer, *FF* of bare PSCs is even higher than that of PSCs with PiG after 1 hour – long UV irradiation. [27] However, as PSCs are irradiated with UV over 1 hour, more PbI_2 is formed and the photovoltaic performance of bare PSCs start to decrease quickly. Liu *et al.* demonstrated that the degradation of perovskite layer can be accelerated by PbI_2 under illumination due to the photodecomposition of PbI_2. [26] In contrast, high UV stability is observed in PSC/PiG, since the down-conversion of PiG prevents the photocatalytic reaction of TiO_2. PCE of PSCs with PiG is 9.09 % after 100 hr - long UV light irradiation. This is much higher than 2.05 % of bare PSC which is UV-irradiated without PiG plate for 100 hrs.

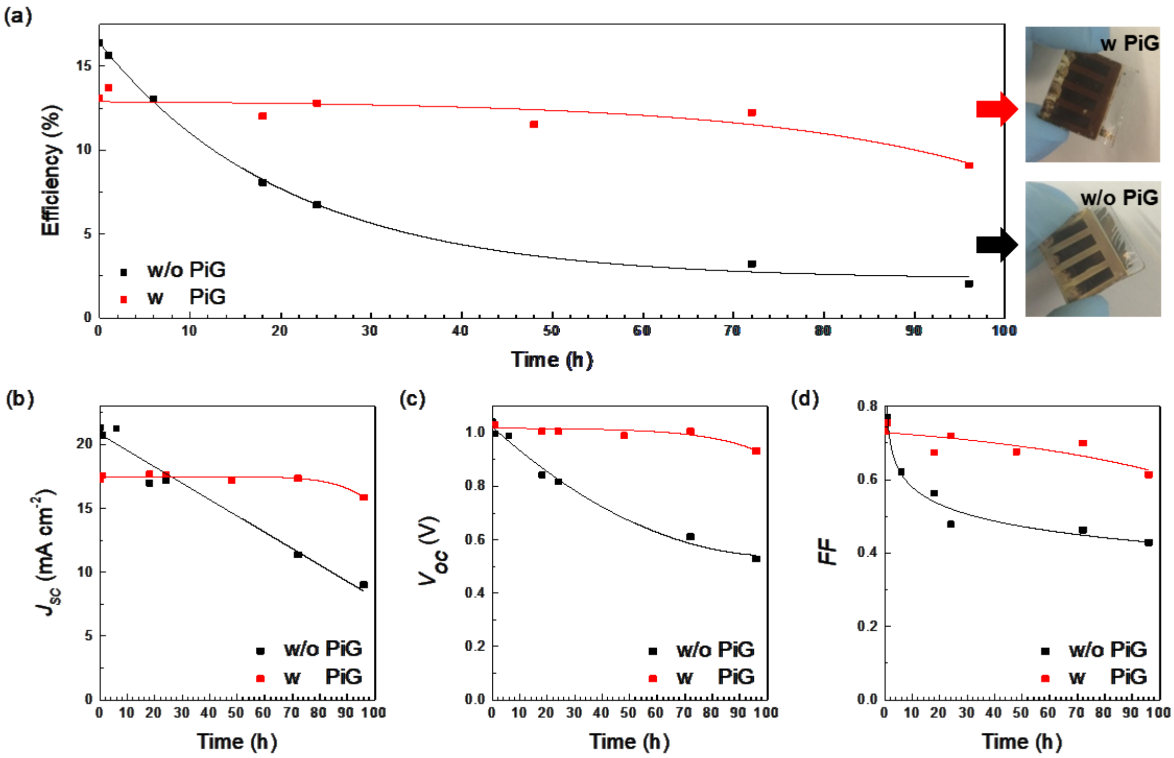

Figure 3. Stability test results of PSCs exposed 365 nm light for 96 hours without and with PiG: (a) efficiency and pictures of PSCs after test without (lower) / with PiG (upper), (b) J_{SC}, (b) V_{OC} and (d) *FF*.

Compared with down-converters in previous studies, we also find that PiG more effectively protects PSCs from UV irradiation damage. When $YVO_3:Eu^{3+}$ nanophosphors and $Au/Y_2O_3:Eu^{3+}$ nanophosphors were used as a down-converter, PCE of PSCs decreased to 60 % and 40 % of the initial PCE after PSCs were irradiated for 12 hour and 24 hour at AM 1.5G illumination (UV light power: 9.2 mW cm^{-2}). [16,17] Given that UV light power (78 mW cm^{-2}) in this study is much higher than UV light power of simulated solar light at AM 1.5G illumination, PiG shows much better UV cut-off ability than nanophosphors of previous studies. This high down-conversion performance of PiG is due to larger particle size and excellent photostability of PiG consisting of micrometer large phosphor particles and glass matrix. Since the particle size of phosphors in PiG is much larger than that of nanoparticle down-converters, PiG absorbs UV light more effectively than the nanohosphors. [28] In addition, the photostability of PiG is better than that of nanophosphors, since the micrometer larger phosphors of PiG has a smaller surface area and the glass matrix passivate the surface. The oxidation reaction can occur on the surface of the phosphors in air. [18,19] Photodegradation of PiG and $YVO_3:Eu^{3+}$ nanophosphor under UV irradiation is shown in Figure 4. While PL intensity of PiG drops only 4 % after 3 hour irradiation, PL intensity of $YVO_3:Eu^{3+}$ nanophosphor decreases by 30 %. During UV irradiation, the oxidation state of V^{5+} changes to V^{4+}. The reduction of transition metal ions induces the formation of an interband defects that act as a luminescence quencher site. This, in turn, decreases the quantum efficiency of nanophosphors. [29] Less effective down-conversion of UV light by aged nanophosphors allows partial transmittance of UV light which weakens the stability of PSCs.

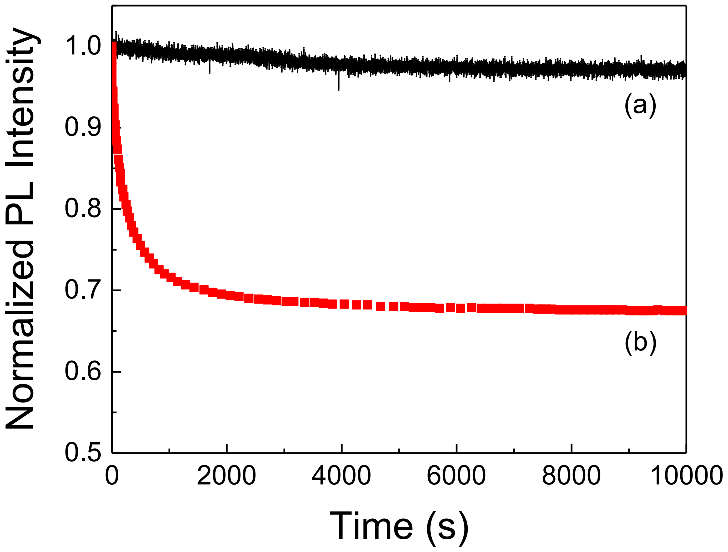

Figure 4. Photostability of (a) PiG, and (b) $YVO_3:Eu^{3+}$ nanophosphor annealed at 300 ºC (Data extracted from Ref. [28]).

4. Conclusion

We demonstrate that PiG enhances stability of PSCs under UV light. 365 nm UV irradiation decomposes $CH_3NH_3PbI_3$ into PbI_2 and gas byproducts and dramatically degrades PCE of PSCs. However, when UV light is irradiated through PiG plate first before reaching the perovskite layer, PSCs maintain their photovoltaic performance for 76 hours. Since PiG converts UV light to visible light, PSCs with PiG not only filters UV light but also harvest the energy of UV light. After 100 hr long UV irradiation, PCE of PSCs with PiG (9.09 %) exceeds that of bare PSCs (2.05 %). In addition, since the glass matrix of PiG passivates the micrometer size phosphor, UV absorption capability and photostability of PiG are better than those of nanophosphor down-converters in literature. This indicates that PiG is an excellent down-converter and an alternative glass substrate which enhances the stability of PSCs under UV light without sacrificing their PCE.

Declarations of interest: none

Acknowledgement

This work was supported from the Global Frontier R&D Program on Center for Multiscale Energy System, Korea (2012M3A6A7054855) and National Science Foundation (Grant No. NSF 1709307).

References

[1] H. Zhou, Q. Chen, G. Li, S. Luo, T. Song, H. Duan, Z. Hong, J. You, Y. Liu, Y. Yang, Interface engineering of highly efficient perovskite solar cells, Science 345 (2014) 542-546.

[2] O. Malinkiewicz, A. Yella, Y. Lee, G. Espallargas, M. Graetzel, M. Nazeeruddin, H. Bolink, Perovskite solar cells employing organic charge-transport layers, Nat. Photonics 8 (2014) 128-132.

[3] H. Yuan, J. Li, M. Wang, Recent progress in research on solid organic-inorganic hybrid solar cells, Acta Phys. Sin. 64 (2015) 038405.

[4] J. Cui, H. Yuan, J. Li, X. Xu, Y. Shen, H. Lin, M. Wang, Recent progress in efficient hybrid lead

halide perovskite solar cells, Sci. Technol. Adv. Mater. 16 (2015) 036004.

[5] W. Yang, J. Noh, N. Jeon, Y. Kim, S. Ryu, J. Seo, S. Seok, High-performance photovoltaic perovskite layers fabricated through intramolecular exchange, Science 348 (2015) 1234-1237.

[6] J. Gong, S. Darling, F. You, Perovskite photovoltaics: life-cycle assessment of energy and environmental impacts, Energy Environ. Sci. 8 (2015) 1953-1968.

[7] N. Espinosa, L. Serrano-Lujan, A. Urbina, F.C. Krebs, Solution and vapour deposited lead perovskite solar cells: Ecotoxicity from a life cycle assessment perspective, Sol. Energy Mater. Sol. Cells 137 (2015) 303-310.

[8] K. Cao, H. Li, S. Liu, J. Cui, Y. Shen, M. Wang, $MAPbI_{3-x}Br_x$ mixed halide perovskites for fully printable mesoscopic solar cells with enhanced efficiency and less hysteresis, Nanoscale 8 (2016) 8839-8846.

[9] S. Ito, S. Tanaka, K. Manabe, H. Nishino, Effects of Surface Blocking Layer of Sb_2S_3 on Nanocrystalline TiO_2 for $CH_3NH_3PbI_3$ Perovskite Solar Cells, J. Phys. Chem. C 118 (2014) 16995-17000.

[10] W. Li, H. Dong, L. Wang, N. Li, X. Guo, J. Li, Y. Qiu, Montmorillonite as bifunctional buffer layer material for hybrid perovskite solar cells with protection from corrosion and retarding recombination, J. Mater. Chem. A 2 (2014) 13587-13592.

[11] H. Cho, S. Jeong, M. Park, Y. Kim, C. Wolf, C. Lee, J. Heo, A. Sadhanala, N. Myoung, S. Yoo, S. Im, R. Friend, T. Lee, Overcoming the electroluminescence efficiency limitations of perovskite light-emitting diodes, Science 350 (2015) 1222-1225.

[12] K. Lim, S. Ahn, Y. Kim, Y. Qi, T. Lee, Universal energy level tailoring of self-organized hole extraction layers in organic solar cells and organic–inorganic hybrid perovskite solar cells, Energy Environ. Sci. 9 (2016) 932-939.

[13] H. Kim, K. Lim, T. Lee, Planar heterojunction organometal halide perovskite solar cells: roles of interfacial layers, Energy Environ. Sci. 9 (2016) 12-30.

[14] T. Leijtens, G. Eperon, S. Pathak, A. Abate, M. Lee, H. Snaith, Overcoming ultraviolet light instability of sensitized TiO_2 with meso-superstructured organometal tri-halide perovskite solar cells,

Nat. Commun. 4 (2013) 2885.

[15] G. Griffini, F. Bella, F. Nisic, C. Dragonetti, D. Roberto, M. Levi, R. Bongiovanni, S. Turri, Multifunctional Luminescent Down-Shifting Fluoropolymer Coatings: A Straightforward Strategy to Improve the UV-Light Harvesting Ability and Long-Term Outdoor Stability of Organic Dye-Sensitized Solar Cells, Adv. Energy Mater. 5 (2015) 1401312.

[16] N. Chander, A. Khan, P. Chandrasekhar, E. Thouti, S. Swami, V. Dutta, V. Komarala, Reduced ultraviolet light induced degradation and enhanced light harvesting using $YVO_4:Eu^{3+}$ down-shifting nano-phosphor layer in organometal halide perovskite solar cells, Appl. Phys. Lett. 105 (2014) 033904.

[17] C.W. Kim, T.Y. Eom, I.S. Yang, B.S. Kim, W.I. Lee, Y.S. Kang, Y.S. Kang, Dual-Function $Au@Y_2O_3:Eu^{3+}$ Smart Film for Enhanced Power Conversion Efficiency and Long-Term Stability of Perovskite Solar Cells, Sci. Rep. 7 (2017) 6849.

[18] Y. Kamiyama, T. Hiroshima, T. Isobe, T. Koizuka, S. Takashima, Photostability of $YAG:Ce^{3+}$ Nanophosphors Synthesized by Glycothermal Method, J. Electrochem. Soc. 157 (2010) J149-J154.

[19] T. Muto, S. Takeshita, T. Isobe, T Sawayama, S. Niikura, Photobleaching Properties of $YVO_4:Eu^{3+}$ Nanophosphors Synthesized by Hydrothermal Treatment, ECS Trans. 16(31) (2009) 135-140.

[20] R. Zhang, H. Lin, Y. Yu, D. Chen, J. Xu, Y. Wang, A new-generation color converter for high-power white LED: transparent Ce^{3+}:YAG phosphor-in-glass, Laser Photonics Rev. 8 (2014) 158-164.

[21] S. Fujita, A. Sakamoto, S. Tanabe, Luminescence Characteristics of YAG Glass–Ceramic Phosphor for White LED, IEEE J. Sel. Top. Quantum Electron. 14 (2008) 1387-1391.

[22] T. Nakanishi, S. Tanabe, Novel Eu^{2+}-Activated Glass Ceramics Precipitated With Green and Red Phosphors for High-Power White LED, IEEE J. Sel. Top. Quantum Electron. 15 (2009) 1171-1176.

[23] A. Shalava, B.S. Richards, T. Trupke, Application of $NaYF_4:Er^{3+}$ up-converting phosphors for enhanced near-infrared silicon solar cell response, Appl. Phys. Lett. 86 (2005) 013505.

[24] N. Ahn, D.-Y. Son, I.-H. Jang, S.M. Kang, M. Choi, N.-G. Park, Highly Reproducible Perovskite Solar Cells with Average Efficiency of 18.3% and Best Efficiency of 19.7% Fabricated via Lewis

Base Adduct of Lead(II) Iodide, J. Am. Chem. Soc. 137 (2015) 8696-8699.

[25] N. Narendran, Y. Gu, J.P. Freyssinier-Nova, Y. Zhu, Extracting phosphor-scattered photons to improve white LED efficiency, Phys. Status Solidi A 202 (2005) R60-R62.

[26] F. Liu, Q. Dong, M.K. Wong, A.B. Djurišić, A. Ng, Z. Ren, Q. Shen, C. Surya, W.K. Chan, J. Wang, A.M.C. Ng, C. Liao, H. Li, K. Shih, C. Wei, H. Su, J. Dai, Is Excess PbI_2 Beneficial for Perovskite Solar Cell Performance?, Adv. Energy Mater. 6 (2016) 1502206.

[27] T. Du, C.H. Burgess, J. Kim, J. Zhang, J.R. Durrant, M.A. McLachlan, Formation, location and beneficial role of PbI_2 in lead halide perovskite solar cells, Sustainable Energy Fuels 1 (2017) 119-126.

[28] S. Arjoca, E.G. Víllora, D. Inomata, Y. Arai, Y. Cho, T. Sekiguchi, K. Shimamura, High homogeneity, thermal stability and external quantum efficiency of Ce:YAG single-crystal powder phosphors for white LEDs, J. Ceram. Soc. Jpn. 124 (2016) 574-578.

[29] Y. Iso, S. Takeshita, T. Isobe, Effects of Annealing on the Photoluminescence Properties of Citrate-Capped $YVO_4:Bi^{3+},Eu^{3+}$ Nanophosphor, J. Phys. Chem. C 118 (2014) 11006-11013.